Incorporation of Aluminium and Iron into the Zeolite MCM-58

Gabriela Košová,[a] Stefan Ernst,[b] Martin Hartmann,[b] and Jiří Čejka*[a]

Keywords: Acidity / Aluminum / Iron / Kinetics / Zeolites

The hydrothermal synthesis of zeolite MCM-58 is investigated with *N*-benzylquinuclidinium bromide as a structure-directing agent in order to isomorphously substitute aluminium or iron for silicon. Al-MCM-58 was synthesised in a wide range of n_{Si}/n_{Al} ratios (from 19 to 56), and Fe-MCM-58 was successfully prepared in a narrower range of n_{Si}/n_{Fe} ratios (from 18 to 36). The obtained products were characterised by XRD, SEM, ^{27}Al MAS NMR, ^{29}Si MAS NMR, FTIR, and ESR spectroscopy. Two different calcination procedures, viz. in a stream of nitrogen and air or in a stream of ammonia, were used in order to modify the acid sites in the zeolite. FTIR spectroscopy before and after the adsorption of [D_3]acetonitrile and pyridine was employed to determine the concentration and type of the acid sites. The acid forms of Al(Fe)-MCM-58 are characterised by the vibrations of bridging Si–OH–Al(Fe) groups at 3628 cm^{-1} and 3564 cm^{-1} (Al-MCM-58) or 3646 cm^{-1} and 3520 cm^{-1} (Fe-MCM-58). The acid sites of both zeolites Al-MCM-58 and Fe-MCM-58 are accessible for [D_3]acetonitrile and pyridine, and all materials contain substantial numbers of Lewis sites (Al-MCM-58: 50 % of the total acid sites; Fe-MCM-58: 90 %) over the whole range of n_{Si}/n_{Al} (n_{Si}/n_{Fe}) ratios studied. Only a small increase in the concentration of Brønsted acid sites was achieved after calcination of the as-synthesised samples in a flow of ammonia.

Introduction

Zeolite-based molecular sieves are a very important group of inorganic materials with a variety of applications, such as adsorption, ion-exchange and, particularly, heterogeneous catalysis.[1,2] The catalytic activity and selectivity of zeolites is attributed to their large internal surface, with active sites that are accessible through uniformly sized pores. The shape and the size of the pore system influence the diffusion of reactants and products and also the path of the reaction. The successful substitution of trivalent heteroatoms into the silicate framework results in a negative charge compensated by protons that are essential for the catalytic activity of zeolites in acid-catalysed reactions. The hydrophobic/hydrophilic properties of high silica zeolites can be varied enormously by suitable variation of the concentration and location of the trivalent cations. Several detailed studies of the feasibility of trivalent cation incorporation into zeolite frameworks, the distribution of these cations among different sites and the location of the charge compensating metal cations in high silica zeolites have been reported that combine experimental and theoretical approaches.[3–6] In the past decade, isomorphous substitution of trivalent cations into various zeolite structures has been reported.[7,8] In addition to aluminosilicate zeolite, ferrisilicate analogues have already been commercially applied as catalysts.[9] Ferrisilicates are less acidic than aluminosilicates, which results in improved selectivity in some acid-catalysed reactions, such as oligomerisation of C_2-C_4 olefins and catalytic dewaxing. Ferrisilicate analogues of molecular sieves can also serve as precursors for the preparation of redox catalysts with a homogeneous distribution of active iron oxide particles, for example in the synthesis of phenol from benzene.[10]

Nowadays, more than 130 framework types have been described[11] and it is still a big challenge to rationally design the synthesis of new structural types of zeolites.[12] The synthesis of zeolites is usually performed under hydrothermal conditions in the presence of various organocationic structure-directing agents (SDA). It is believed that the size and shape of the SDA predefine the shape and dimensions of the zeolite pore system.[13] The synthesis efforts using novel types of SDA in many laboratories around the world have resulted recently in the successful synthesis of new types of zeolites, for example ITQ-21, a large-pore, three-dimensional zeolite,[14] ITQ-13, with 9- and 10-membered rings,[15] a zeolite having 8-, 10- and 12-membered rings,[16] SSZ-58, a zeolite with previously unseen double 5-ring subunits,[17] MCM-68, in which 12-membered-rings channel are intersected by two independent tortuous 10-membered-ring channel systems,[18] or the novel, extra-large-pore zeolites SSZ-53 and SSZ-59, which possess 14-membered rings in a one-dimensional channel system.[19] Other strategies have been developed for the synthesis of micro/meso-composite molecular sieves.[20,21]

[a] J. Heyrovský Institute of Physical Chemistry, Academy of Sciences of the Czech Republic,
Dolejškova 3, 182 23 Prague, Czech Republic
Fax: +420-28658-2307
E-mail: jiri.cejka@jh-inst.cas.cz
[b] Department of Chemistry, Chemical Technology, University of Kaiserslautern,
Erwin-Schrödinger-Strasse 54, 67663 Kaiserslautern, Germany

  DOI: 10.1002/ejic.200400743

Zeolite MCM-58, which was described for the first time in 1994 by Valyocsik as a high-silica zeolite, can be synthesised with n_{Si}/n_{Al} ratios from 15 to 50.[22] Zeolite MCM-58 (IZA structure code IFR) is isostructural with SSZ-42 and ITQ-4 and is characterised by an undulating, one-dimensional, 12-membered-ring channel system.[23] Due to the relatively large pore diameter of 0.64 nm at the narrowest point and a cage at the widest point with a diameter of 1.0 nm, zeolite MCM-58 could be an interesting catalyst for the conversion of relatively bulky molecules. For example, MCM-58 has been used as catalyst in the gas-phase alkylation of toluene with propylene giving large amount of *n*-propyltoluenes,[24] or ethylbenzene disproportionation and hydroconversion of *n*-decane.[25] Several organic SDAs have been used for the synthesis of MCM-58, including benzyltropanium salts, *N*-benzyl-1-azabicyclo[2.2.2]octane cations (benzylquinuclidinium) and *N*-benzyl-1,4-diazabicyclo[2.2.2] cations.[22]

In the present work, we report on the synthesis of aluminosilicate MCM-58 with n_{Si}/n_{Al} ratios from 20 to 60 and of ferrisilicate MCM-58 with n_{Si}/n_{Fe} ratios from 20 to 40 using *N*-benzylquinuclidinium bromide (BQ) as the templating agent. In particular, we were interested in the isomorphous substitution of iron for silicon in the framework of MCM-58, which has not yet been described. The kinetics of the crystallisation and the effect of incorporated trivalent atoms on concentrations and types of acid sites of this zeolite were also investigated.

Results and Discussion

The progress of crystallisation of MCM-58 from molar gel compositions of $(0.016–0.025)\,Al_2O_3$:SiO_2:$38\,H_2O$:$0.30\,K_2O$:$0.10\,BQ$ for Al-MCM-58 and $(0.0125–0.025)\,Fe_2O_3$:SiO_2:$38\,H_2O$:$0.30\,K_2O$:$0.20\,BQ$ for Fe-MCM-58 was followed by X-ray powder diffraction. By optimising the synthesis conditions and time at 170 °C it was possible to reproducibly synthesise highly crystalline zeolite Al-MCM-58 (Figure 1) with initial n_{Si}/n_{Al} ratios from 20 to 60. Because BQ, which is used as an SDA in the synthesis of MCM-58, is relatively expensive, the amount of BQ in the reaction mixture for Al-MCM-58 was further lowered from the original BQ/SiO_2 molar ratio of 0.2 to 0.1. Even with a reduced amount of SDA, MCM-58 can be synthesised without any loss of quality. When the BQ/SiO_2 ratio is lower then 0.1, or BQ is omitted completely, α-quartz is obtained as a pure phase.[26] A similar effect occurs when the amount of aluminium in the reaction mixture is decreased. When the initial n_{Si}/n_{Al} ratio exceeds 60, α-quartz begins to crystallise as well. Valyocsik has reported that mordenite can be formed as an impurity phase if either the n_{Si}/n_{Al} ratio is less then 10 in the initial gel or sodium cations are used instead of potassium cations in the synthesis gel.[27]

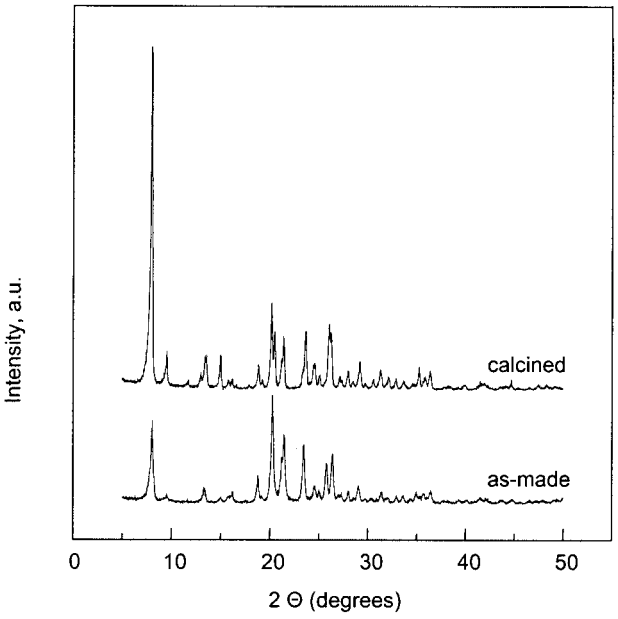

Figure 1. X-ray powder-diffraction patterns of as-synthesised and calcined Al-MCM-58 (n_{Si}/n_{Al} = 36).

The MCM-58 reflections were first observed after three days of synthesis (Figure 2) and the crystallisation was complete after six to eight days, depending on the n_{Si}/n_{Al} ratio (n_{Si}/n_{Al} = 60, 40, 30 and 20, respectively). The rate of crystallisation increases with decreasing amount of aluminium. A relative decrease in the crystallisation rate with reduced aluminium concentration in the synthesis gel has also been reported for other zeolites, such as Al-ZSM-12.[28]

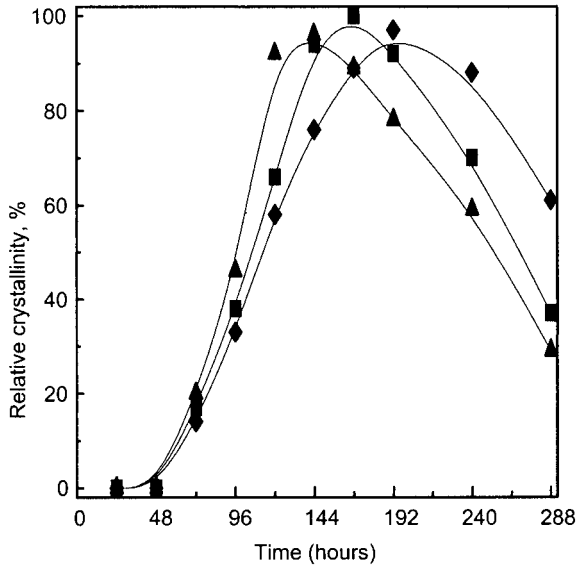

Figure 2. The dependence of relative crystallinity of Al-MCM-58 on the initial n_{Si}/n_{Al} ratio. Temperature: 170 °C; n_{Si}/n_{Al} = 20 (▲), 30 (■), 40 (♦).

In contrast to the synthesis of Al-MCM-58, which was carried out at 170 °C and yielded the phase-pure zeolite, in the case of Fe-MCM-58 it was not possible to synthesise

this zeolite as a pure phase under the same conditions: the sample was always contaminated with α-quartz. After six days, α-quartz was the sole product (see Figure 3). To prevent the formation of α-quartz, the reaction temperature for the synthesis of Fe-MCM-58 was lowered to 155 °C and the synthesis time was optimised. The optimal synthesis time was found to be between 4.5 and 5.5 days independent of the n_{Si}/n_{Fe} ratio in the gel. The molar ratio BQ/SiO_2 was kept at 0.2 as in the original recipe for Al-MCM-58. It was not possible to lower it as in the synthesis of Al-MCM-58. Under these conditions, pure Fe-MCM-58 was synthesised. Moreover, we found that the silicon source is of uttermost importance in order to obtain phase-pure Fe-MCM-58. Three different silica sources were tested, namely Ludox AS-30, Ludox AM-30 and Levasil, all of them as 30 wt-% SiO_2 solutions in water. Phase-pure zeolite Fe-MCM-58 was obtained only with Levasil as the silica source (Figure 3). The shape of the crystallisation curves (Figure 4) reveals that crystallisation starts after two days and increases to 70–80% after 96 h. The crystallisation curves for Fe-MCM-58 are characterised by a sharp maximum at about 120 h irrespective of the n_{Si}/n_{Fe} ratio. Thereafter, α-quartz starts to be formed as well, and later on Fe-MCM-58 is completely transformed into α-quartz, which is the thermodynamically most stable phase. The zeolite synthesis obeys the Ostwald ripening law. As described for zeolite A, the initial metastable phase is converted into a thermodynamically more stable sodalite until the most stable SiO_2 is formed.[29] Thus, the successful synthesis of Fe-MCM-58 requires the control of the optimum synthesis time, which was found to be close to 5.5 days for the conditions used (Figure 5).

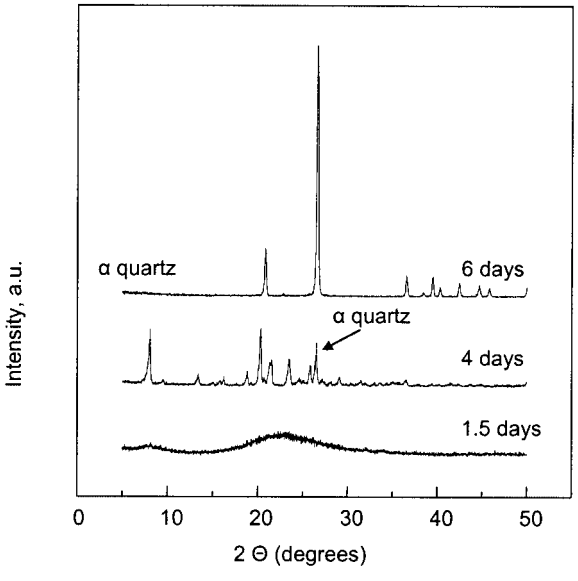

Figure 3. X-ray powder diffraction pattern of Fe-MCM-58 (n_{Si}/n_{Fe} = 28, T = 170 °C). After six days α-quartz is formed.

The scanning electron micrographs (Figure 6) of Al-MCM-58 (n_{Si}/n_{Al} = 36) and Fe-MCM-58 (n_{Si}/n_{Fe} = 36) show that no amorphous phase is present. Crystals of Al-

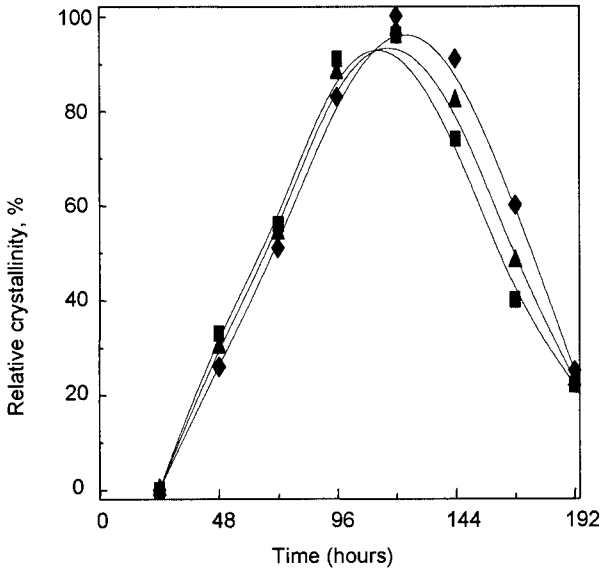

Figure 4. The dependence of relative crystallinity of Fe-MCM-58 on the initial n_{Si}/n_{Fe} ratio. Temperature: 155 °C; n_{Si}/n_{Fe} = 20 (▲), 30 (■), 40 (♦).

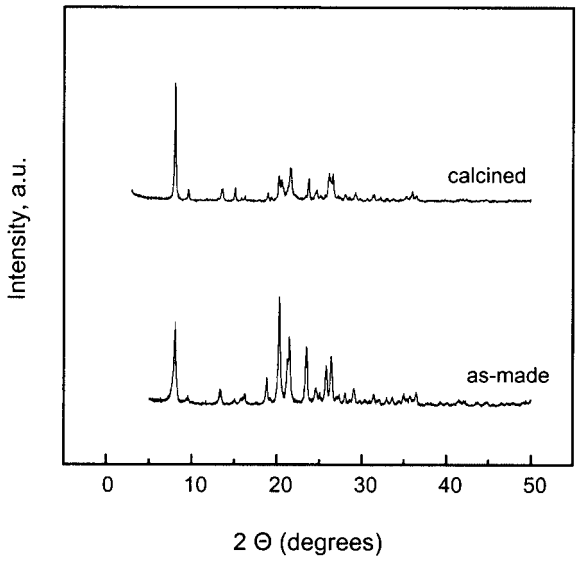

Figure 5. X-ray powder-diffraction pattern of Fe-MCM-58 (n_{Si}/n_{Fe} = 28; T = 155 °C; crystallisation time: 5 days).

MCM-58 (A and B) are represented by elongated particles with lengths ranging from 1 to 5 μm depending on the n_{Si}/n_{Al} ratio in the synthesis gel. The size of the crystals increases with a decreasing amount of aluminium in the reaction mixture. No uniform distribution of crystal sizes was observed for Al-MCM-58. The crystals of Fe-MCM-58 (n_{Si}/n_{Fe} = 36) (see C,D in Figure 6) are smaller than those of Al-MCM-58, with sizes between 0.5 and 3.0 μm. Some agglomeration of Fe-MCM-58 crystals to form stars was found (see C in Figure 6), which is also typical for Fe-ZSM-12.[28]

In agreement with our previous data,[25,31] two resonance signals at about δ = 58 and 61 ppm, reflecting tetrahedrally coordinated Al atoms, are observed in the ^{27}Al MAS NMR

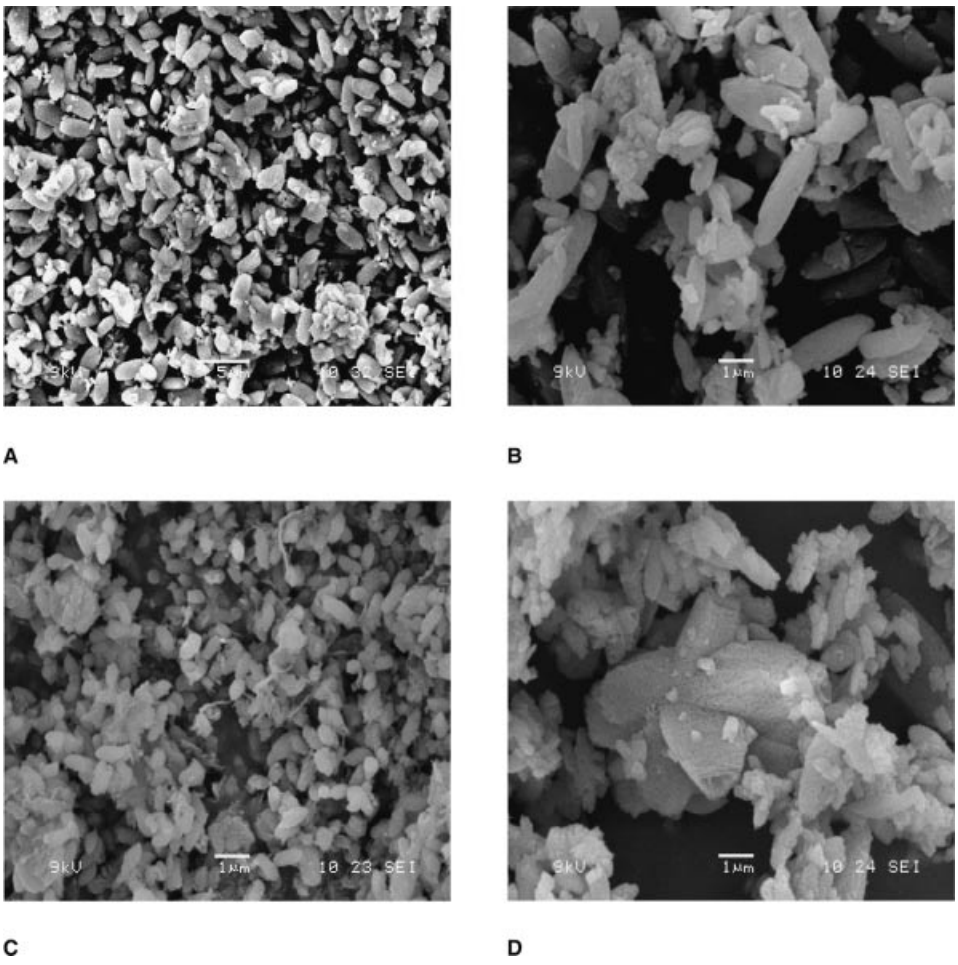

Figure 6. Scanning electron micrographs of zeolites Al-MCM-58 (A, B) and Fe-MCM-58 (C, D).

spectra of Al-MCM-58 with n_{Si}/n_{Al} ratios from 19 to 56 (Figure 7). No resonance around δ = 0 ppm, corresponding to octahedrally coordinated aluminium at extra-framework positions, was observed. This indicates that only tetrahedrally coordinated aluminium is present in Al-MCM-58. The two resonances in the tetrahedral region are explained by the presence of two crystallographically inequivalent aluminium atoms in T1–T4 sites.[31,37] The relative amount of the two different kinds of aluminium (δ = 60.9 and 58.2 ppm) changes with the n_{Si}/n_{Al} ratio: with increasing amount of aluminium in the zeolite, the intensity of the resonance at δ = 60.9 ppm decreases.

The ^{29}Si NMR spectrum of Al-MCM-58 (n_{Si}/n_{Al} ratio = 56) is composed of two broad, complex bands centred around δ = –110 and –102 ppm corresponding to tetrahedrally coordinated silicon atoms with different local environments (see a in Figure 8). The band around δ = –110 ppm can be attributed to Si(4Si) atoms, and is a superposition of four resonances at δ = –107.7, –109.3, –110.7 and –111.8 ppm. These resonances correspond to Si(4Si) atoms at four crystallographically inequivalent positions (T1–T4). The observed chemical shifts are in good agree-

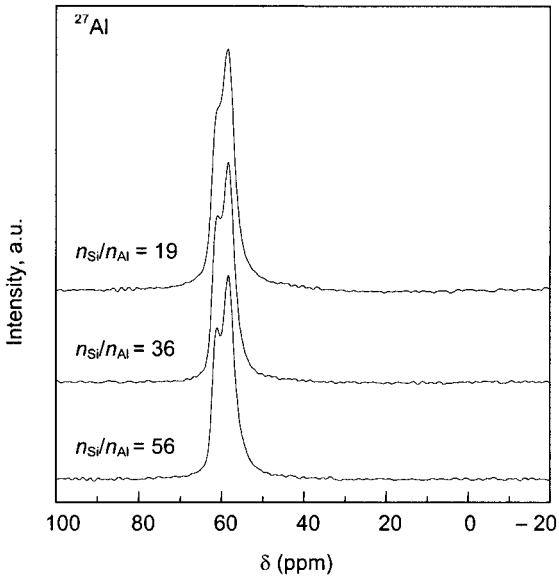

Figure 7. ^{27}Al MAS NMR spectra of Al-MCM-58 samples with different n_{Si}/n_{Al} ratios.

ment with those reported for ITQ-4, which is isostructural with MCM-58 (δ = –108.0, –109.7, –110.9 and –111.5 ppm).[30] The higher resolution of the ^{29}Si NMR spectrum of Al-MCM-58 than that in the literature[31,37] is explained by the decrease in the perturbation of the Si environment due to a lower framework aluminium content. The broad band centred at δ = –102 ppm is ascribed to a superposition of the resonances corresponding to Si(3Si, 1Al) atoms and Si(3Si,OH) atoms. Decomposition of the spectrum to the Gaussian curves (not shown) indicated the presence of two resonances at δ = –101.1 and –104.0 ppm. The resonance at δ = –101.1 ppm can be attributed to Si(3Si, OH) atoms, as indicated by a CP experiment (see a in Figure 8). The resonance at δ = –104.0 ppm corresponds to Si(3Si, 1Al) atoms. Note that the intensity correction factor of Si(3Si, OH) is 1, compared to a value of 0.25 for Si(3Si, 1Al). Thus the relatively high intensity of the resonance at δ = –101.1 ppm compared to that at δ = –104.0 ppm indicates a higher amount of silanol groups than framework Al in the sample. A high amount of silanol groups has also been reported in previous papers from Ernst et al.[31,37]

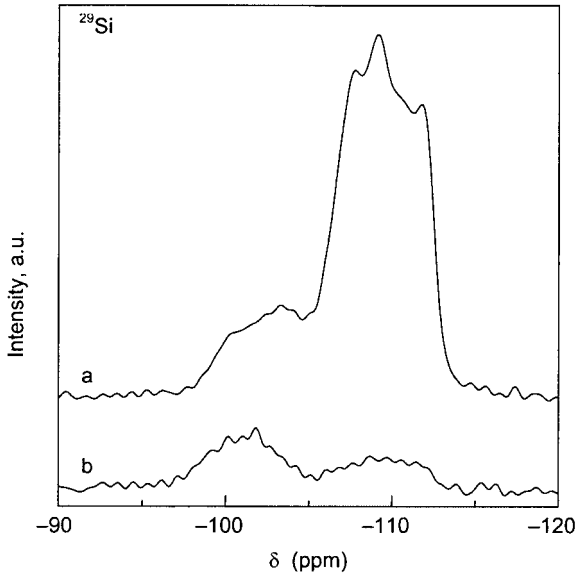

Figure 8. ^{29}Si HP (a) and CP (b) MAS NMR spectra of hydrated Al-MCM-58 (n_{Si}/n_{Al} = 56).

The type and concentration of the acid sites were determined after adsorption of probe molecules such as [D_3]acetonitrile and pyridine on the activated zeolites Al-MCM-58 and Fe-MCM-58, respectively. The spectra of Al-MCM-58 in the region of OH groups before and after adsorption of [D_3]acetonitrile are depicted in part A of Figure 9. The absorption band at 3746 cm^{-1} belongs to terminal Si–OH groups and the two bands at 3630 and 3564 cm^{-1} are characteristic of bridging OH groups. After the interaction with [D_3]acetonitrile, the bands of the hydroxyls groups are significantly reduced and new bands at 2327 cm^{-1} (Lewis sites) and 2297 cm^{-1} (Brønsted sites) are formed (see B in Figure 9).

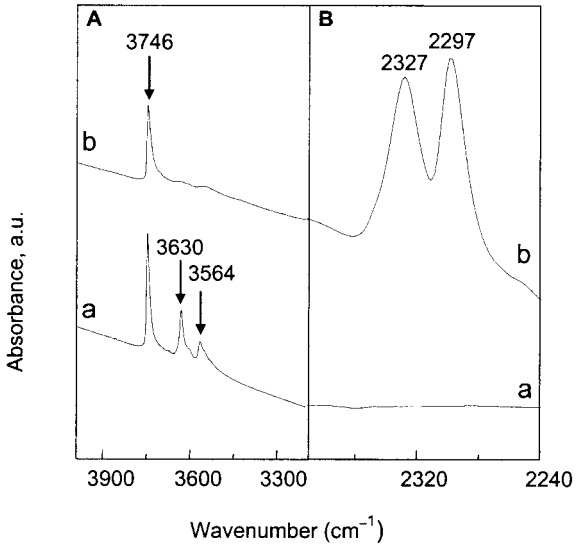

Figure 9. IR spectra of hydroxyl vibration region of Al-MCM-58 with n_{Si}/n_{Al} = 36 before (a) and after (b) [D_3]acetonitrile adsorption (A) and spectra of acetonitrile region before (a) and after (b) its adsorption (B).

In the case of Fe-MCM-58, absorption bands with maxima at 3746 cm^{-1} for terminal Si–OH groups and 3646 and 3520 cm^{-1} for bridging Si–OH–Fe groups (see A,a in Figure 10) were detected. Pyridine adsorption leads to the consumption of all bridging Si–OH–Fe groups (see A,b in Figure 10) and the formation of a band at 1545 cm^{-1} characteristic of the presence of the pyridinium ion, which reflects the interaction of pyridine with Brønsted sites. The band at 1448 cm^{-1} originates from coordinatively bonded pyridine on Lewis sites (see B,b in Figure 10).

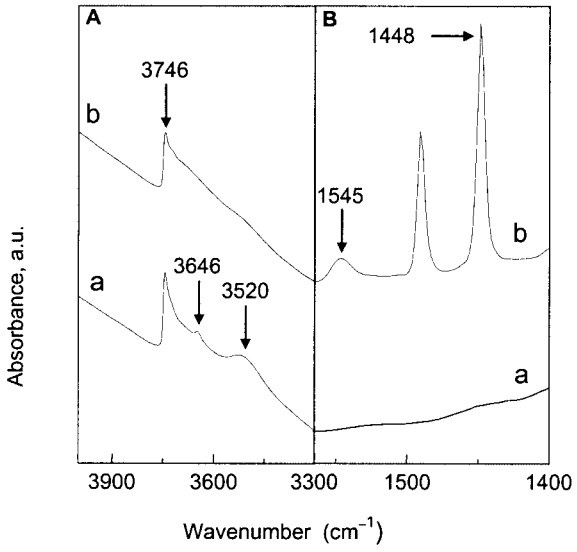

Figure 10. IR spectra of hydroxyl vibration region of Fe-MCM-58 with n_{Si}/n_{Fe} = 28 before (a) and after (b) pyridine adsorption (A) and spectra of pyridine region before (a) and after (b) its adsorption (B).

The type, strength and concentration of acid sites control the rate and pathway of acid-catalysed reactions such as hydrocarbon cracking and rearrangement. It is evident that Lewis and Brønsted acid sites play a role in catalytic processes; however, their role is still not completely clear. In *n*-butene skeletal isomerisation, it has been shown that an increasing concentration of Lewis sites enhances the rate of deactivation.[32] We tried to modify the concentration of different types of acid sites in MCM-58 by using different methods of calcination. Besides the classical two-step calcination procedure in a stream of nitrogen and air at a calcination temperature of 540 °C, calcination in a stream of ammonia at a temperature of 450 °C was also used. The latter procedure has been described for zeolite beta by Kunkeler et al.,[33] who showed that this treatment results in a reduced formation of Lewis acid sites. They supposed that ammonia ions substitute the leaving organic template cations occluded in the channel system of the zeolite and thus stabilise the zeolite structure. Furthermore, Bourgeat-Lami et al.[34] have proposed that ammonium cations could hinder the formation of octahedrally coordinated aluminium and thus stabilise the structure of the zeolite. In the case of Al-MCM-58 (n_{Si}/n_{Al} = 19), the relative concentration of Brønsted acid sites amounts to about 47% and that of Lewis acid sites to bout 53%. After calcination of this zeolite in a stream of ammonia (5% of NH_3 in N_2) the relative concentration of Brønsted sites increased to 53%. Similar trends were also observed for Fe-MCM-58 (Table 1).

Table 1. n_{Si}/n_{Al} and n_{Si}/n_{Fe} ratios of zeolites Al-MCM-58 and Fe-MCM-58 in the initial gel and in the synthesised zeolite, as determined by X-ray fluorescence (XRF) and FTIR spectroscopy, and the relative amounts of Lewis and Brønsted acid sites.

Calcination	Si/Al[a]	Si/Al (XRF)	Si/Al (FTIR)	LS [%][b]	BS [%][b]
calcd. N_2/air	20	19	19	53	47
	40	36	36	53	47
	60	56	53	55	45
calcd. NH_3	20	19	19	47	53
	40	37	35	48	52
	60	56	52	49	51
Calcination	Si/Fe[a]	Si/Fe (XRF)	Si/Fe (FTIR)	LS [%][c]	BS [%][c]
calcd. N_2/air	20	18	18	86	14
	30	28	27	89	11
	40	36	32	94	6
calcd. NH_3	20	18	18	84	16
	30	28	26	86	14
	40	36	31	92	8

[a] Initial n_{Si}/n_M ratio in the reaction gel. [b] Adsorption of acetonitrile. [c] Adsorption of pyridine.

The determined concentrations of Brønsted and Lewis acid sites for Al- and Fe-MCM-58 are summarised in Table 1. From a comparison of the n_{Si}/n_{Al} (n_{Si}/n_{Fe}) ratios in the initial reaction mixture and in the synthesised zeolite we found that the obtained product was always richer in aluminium (iron) than the initial gel. The increase in the Al (Fe) content in the zeolite is more notable for Fe-MCM-58 than for Al-MCM-58.

The concentration of the Brønsted acid sites in Al-MCM-58 is practically constant despite the n_{Si}/n_{Al} ratio, while it decreases slightly with an increasing n_{Si}/n_{Fe} ratio. In other words, the higher the concentration of trivalent atoms in the zeolite, the higher the concentration of Lewis sites. The concentration of Brønsted sites depends strongly on the type of trivalent cation. While about 50% of the acid sites are of the Brønsted type in the Al-containing MCM-58 samples, only about 8–16% of the total acid sites are Brønsted sites in Fe-MCM-58. On one side, the concentration of trivalent cations in the synthesised sample is larger for Fe than for Al, whereas the concentration of Brønsted sites is significantly lower for Fe-MCM-58 than for Al-MCM-58. Due to the relatively large ionic radius of Fe^{3+} (0.063 nm) compared to Si^{4+} and Al^{3+} (0.040 nm and 0.053 nm,[35] respectively), the incorporation of iron into the framework is expected be much more complicated. Some evidence for the incorporation of iron into the Fe-MCM-58 framework can be obtained from the ESR spectra. The X-band EPR spectra (not shown) recorded at –196 °C for the calcined Fe-MCM-58 materials with different n_{Si}/n_{Fe} ratios show a sharp signal at g = 4.3 with shoulders at g = 9.1 and g = 2.3 and an intense broad signal at g = 2. The relative proportion of the signal at g = 4.3 decreases from n_{Si}/n_{Fe} = 40 to 20. The signal intensity is directly proportional to the iron content in the materials with different n_{Si}/n_{Fe} ratio. The assignment of the EPR signals to various species is still a matter of debate and is beyond the scope of this paper. Details can be found in our subsequent publication.[36]

Conclusions

Zeolite MCM-58 containing trivalent metal cations such as Al and Fe in the framework can be readily synthesised with *N*-benzylquinuclidinium bromide as the structure directing agent and Levasil (30% SiO_2 in water) as the silica source. The synthesis of Al-MCM-58 was accomplished at an SiO_2/BQ concentration of 0.1 in a wide range of initial n_{Si}/n_{Al} ratios (20 to 60) under dynamic conditions at 170 °C.

Incorporation of iron into the zeolite framework is not as straightforward. The synthesis requires a lower temperature, higher concentration of the template, and the suitable range of initial n_{Si}/n_{Fe} ratios is narrower (20 to 40). The synthesis was carried out with a SiO_2/BQ ratio of 0.2, under dynamic conditions at 155 °C.

The acid forms of both Al-MCM-58 and Fe-MCM-58 contain substantial amounts of Brønsted and Lewis acid sites. After calcination in a stream of ammonia, the amount of Brønsted sites was slightly greater than after conventional calcination in nitrogen and air.

Experimental Section

Abbreviations: BQ = *N*-benzylquinuclidinium bromide, CP = cross polarisation.

The syntheses of MCM-58 with n_{Si}/n_{Al} ratios in the initial synthesis gel ranging from 20 to 60 and n_{Si}/n_{Fe} ratios ranging from 20 to 40 were investigated under hydrothermal conditions in Teflon-lined, stainless-steel autoclaves (35 and 90 mL) under autogenous pressure. *N*-Benzylquinuclidinium bromide (BQ) was used as structure-directing agent in a modified version of the procedure for the synthesis of zeolite MCM-58 described previously.[37]

N-Benzylquinuclidinium bromide was prepared by refluxing an equimolar mixture of benzyl bromide (from Fluka) and quinuclidine (from Fluka) in ethanolic solution for 24 h. Crystals were recovered after cooling the reaction mixture in an ice bath. The chemical composition and structure of the template were confirmed by elemental analysis and NMR spectroscopy.

The synthesis gels were prepared in polyethylene beakers at ambient temperature. In a typical synthesis of Al-MCM-58, 3.69 g of $Al_2(SO_4)_3 \cdot 18\,H_2O$ (from Fluka) was dissolved in 88.00 g of distilled water. To this solution, 3.24 g of KOH (from Lachema, CZ) and subsequently 4.02 g of *N*-benzylquinuclidinium bromide (as made) were added whilst stirring. Later on, 30.00 g of colloidal silica sol (30 wt.-% SiO_2 in water, Ludox AS-30, from Aldrich) was added slowly with vigorous stirring to the reaction mixture, which was finally homogenised for 2 min. The resulting gel was loaded into 90-mL, Teflon-lined, stainless steel autoclaves. The synthesis was carried out with agitation at 170 °C for Al-MCM-58 and at 155 °C for Fe-MCM-58 for 4 to 9 days. For the synthesis of Fe-MCM-58, the aluminium source was replaced by $Fe(NO_3)_3 \cdot 9\,H_2O$ (from Fluka) and instead of Ludox AS-30, Levasil VP 4038 (30% SiO_2 in water, from Bayer AG) was used. After crystallisation, the autoclaves were cooled to room temperature by quenching in cold water; the solid product was recovered by filtration, washed with distilled water, and dried at 80 °C overnight.

To remove the template, the as-synthesised sample was heated to 200 °C in a stream of nitrogen with a temperature ramp of 1 °C min^{-1} and kept at the same temperature for 4 h. Thereafter, the sample was heated to 540 °C with the same heating rate and kept for 2 h at this temperature. Finally, the material was calcined for 24 h in a stream of air at 540 °C.

In a second set of experiments the as-synthesised sample was treated in a stream of ammonia at 470 °C for 8 h with a heating rate of 1 °C min^{-1}. The samples were then ion-exchanged twice with a 0.5 M $NaNO_3$ solution for 8 h and once with 1.0 M $NaNO_3$ for 8 h using 100 mL of solution per gram of zeolite at room temperature. Finally, the sample was calcined again as described above.

The ammonium forms of both zeolites were prepared by fourfold repeated ion-exchange of the zeolite in a 0.5 M aqueous solution of ammonium nitrate at ambient temperature.

X-ray powder diffraction was used for identification of as-synthesised zeolites and the determination of their crystallinity to follow the kinetics of the crystallisation process. The XRD patterns were collected on a Siemens D5005 X-ray powder diffractometer equipped with a graphite monochromator and scintillation counter using Cu-K_α radiation in Bragg–Brentano geometry. Relative crystallinity is defined as the intensity of the peak at $2\theta = 20.53°$ compared to that of the MCM-58 sample with the highest crystallinity obtained in this study.

^{29}Si and ^{27}Al MAS NMR experiments were performed on a Bruker Avance 500 MHz (11.7 T) Wide Bore spectrometer operating at Larmor frequencies of 130.3 MHz for aluminium and 99.35 MHz for silicon using 4 mm and 7 mm o.d. rotors, respectively. Prior to the NMR experiments, all calcined samples were ion-exchanged three times with a 0.5 M NaCl solution for 8 h using 100 mL of solution per gram of zeolite at room temperature. In order to monitor Si coordination and local environment in the samples, ^{29}Si MAS NMR high-power decoupling (HPDec) and cross-polarisation (CP) experiments were carried out. In the case of high-power decoupling, pulse sequences with a $\pi/6$ (1.7 μs) excitation pulse and relaxation delay of 30 s were applied. 1024 FIDs were accumulated to obtain a sufficiently good signal-to-noise ratio. In the case of cross-polarisation spectra, pulse sequences with 50% ramp CP pulse, contact time 2 ms, high-power decoupling and a relaxation delay of 5 s were applied. 10 240 FIDs were accumulated to obtain the spectrum. Rotors were spun at a speed of 5 kHz; chemical shifts are referenced to the chemical compound Q8M8 as a standard. ^{29}Si high-power decoupling spectra were decomposed to the Gaussian bands using Microcall Origin 4.1 software (Microcall Software Inc., U.S.A.).

In order to measure the ^{27}Al MAS NMR spectra, high-power decoupling pulse sequences with a $\pi/12$ (0.7 μs) excitation pulse and relaxation delay of 1 s were applied; 1024 FIDs were accumulated to obtain the spectrum. Rotors were spun at a speed of 12 kHz;chemical shifts are referenced to an aqueous solution of $Al(NO_3)_3$.

The shape and the size of zeolite crystals were determined by scanning electron microscopy (JEOL, JSM-03). X-ray fluorescence spectroscopy was employed to estimate the chemical composition of Al- and Fe-MCM-58.

The concentrations of Brønsted and Lewis acid sites in Al-MCM-58 and Fe-MCM-58 were determined after the adsorption of [D_3]-acetonitrile and pyridine, respectively, followed by FTIR spectroscopy using a Nicolet FTIR Protégé 460 spectrometer. For this purpose, the zeolite powders were pressed binder-free into self-supporting wafers with a density from 4.0 to 10.0 mg cm^{-2}. [D_3]Acetonitrile was degassed by repeated freeze-thaw cycles before use. Prior to the adsorption of [D_3]acetonitrile, the zeolites were activated in situ by overnight evacuation at 400 °C. All measured spectra were recalculated to a normalised wafer thickness of 10 mg cm^{-2}. For a quantitative characterisation of the Brønsted acid sites (B), the C≡N–B vibration at about 2296 cm^{-1} was used with an extinction coefficient of $\varepsilon_B = 2.05 \pm 0.1$ cm μmol^{-1}. For a quantitative evaluation of Lewis acid sites (L), the C≡N–L vibration at 2323 cm^{-1} was used with an extinction coefficient of $\varepsilon_L = 3.6 \pm 0.1$ cm μmol^{-1}.[38] To determine the concentrations of acid sites in Fe-MCM-58, pyridine was used as a probe molecule. From the integral intensities of individual bands at 1545 cm^{-1} (Brønsted sites) and at 1448 cm^{-1} (Lewis sites) and using extinction coefficients of $\varepsilon_L = 1.67 \pm 0.1$ and $\varepsilon_B = 2.22 \pm 0.1$ cm μmol, respectively, concentrations of both types of acid sites were calculated according to ref.[39]

Acknowledgments

This study was supported by the Grant Agency of the Czech Republic (203/02/0804) and by the Volkswagen-Stiftung (I/75 886). G. K. thanks the Grant Agency of the Academy of Sciences of the Czech Republic (B4040402). S. E. and M. H. gratefully acknowledge financial support by the Deutsche Forschungsgemeinschaft and the Fonds der Chemischen Industrie. The authors thank Dr. L. Brabec for recording SEM pictures and Dr. J. Dědeček for running the MAS NMR experiments (both J. Heyrovský Institute, Prague).

[1] J. Čejka, B. Wichterlová, *Catal. Rev.* **2002**, *44*, 375–421.

[2] C. S. Cundy, P. A. Cox, *Chem. Rev.* **2003**, *103*, 663–701.
[3] V. Gábová, J. Dědeček, J. Čejka, *Chem. Commun.* **2003**, *10*, 1196–1197.
[4] J. Kučera, P. Nachtigall, *Phys. Chem. Chem. Phys.* **2003**, *15*, 3311–3317.
[5] Q. Li, A. Navrotsky, F. Rey, A. Corma, *Microporous Mesoporous Mater.* **2003**, *64*, 127–133.
[6] J. Yu, J. Li, R. Xu, *Microporous Mesoporous Mater.* **2001**, *48*, 47–56.
[7] G. Bellussi, M. S. Rigutto, *Stud. Surf. Sci. Catal.* **1994**, *85*, 177–213.
[8] G. Perego, R. Millini, G. Bellussi, in *Molecular Sieves: Science and Technology* (Eds.: H. G. Karge, J. Weitkamp), Springer, *Molecular Sieves* **1998**, *1*, 187.
[9] P. Ratnasamy, R. Kumar, *Catal. Today* **1991**, *9*, 329–416.
[10] B. Liptakova, M. Hronec, Z. Cvengrosova, *Catal. Today* **2000**, *61*, 143–148.
[11] W. M. Meier, D. H. Olson, C. Baerlocher, *Atlas of Zeolite Structure Types*, 5th ed., Elsevier, Amsterdam **2001**.
[12] M. Tagliabue, L. C. Carluccio, D. Ghisletti, C. Perego, *Catal. Today* **2003**, *81*, 405–412.
[13] M. E. Davis, F. R. Lobo, *Chem. Mater.* **1992**, *4*, 756–768.
[14] A. Corma, M. Diaz-Cabanas, J. Martinez-Triguero, F. Rey, J. Rius, *Nature* **2002**, *418*, 514–517.
[15] A. Corma, M. Puche, F. Rey, G. Sankar, S. J. Teat, *Angew. Chem. Int. Ed.* **2003**, *42*, 1156–1159.
[16] A. Corma, F. Rey, S. Valencia, J. L. Jorda, J. Ruis, *Nat. Mater.* **2003**, *2*, 493–497.
[17] A. Burton, S. Elomari, R. C. Medrud, I. Y. Chan, C.-Y. Chen, L. M. Bull, E. S. Vittoratos, *J. Am. Chem. Soc.* **2003**, *125*, 1633–1642.
[18] D. C. Calabro et al., *US Patent 6,049,018*, assigned to Mobil Oil Corp **2000**.
[19] A. Burton, S. Elomari, C. Y. Chen, *Chem. Eur. J.* **2003**, *9*, 5737–5748.
[20] P. Prokešová, S. Mintova, J. Čejka, T. Bein, *Microporous Mesoporous Mater.* **2003**, *64*, 165–174.
[21] C. J. H. Jacobsen, C. Madsen, J. Houžvička, *J. Am. Chem. Soc.* **2000**, *122*, 7116–7117.
[22] E. W. Valyocsik, *WO Patent 95/11196* assigned to Mobil Oil Corp. **1994**.
[23] C. Y. Chen, L. W. Finger, R. C. Medrud, C. L. Kibby, P. A. Crozier, I. Y. Chan, T. V. Harris, L. W. Beck, S. I. Zones, *Chem. Eur. J.* **1998**, *4*, 1312–1323.
[24] J. Čejka, A. Krejčí, N. Žilková, J. Kotrla, S. Ernst, A. Weber, *Microporous Mesoporous Mater.* **2002**, *53*, 121–133.
[25] S. Ernst, M. Hartmann, T. Hecht, A. Weber, *Stud. Surf. Sci. Catal.* **2001**, *135*, 315–317.
[26] S. Ernst, in *Molecular Sieves: Science and Technology* (Eds.: H. G. Karge, J. Weitkamp), Springer, *Molecular Sieves*, **1998**, *1*, 66.
[27] E. W. Valyocsik, *US Patent 5,441,721*, assigned to Mobil Oil Corp. **1994**.
[28] G. Košová, J. Čejka, *Collect. Czech. Chem. Commun.* **2002**, *67*, 1760–1778.
[29] J. R. Francis, D. O'Hare, *J. Chem. Soc., Dalton Trans.* **1998**, *19*, 3133–3148.
[30] M. C. Camblor, A. Corma, L. A. Villaescusa, *Chem. Commun.* **1997**, *8*, 749-750.
[31] S. Ernst, M. Hartmann, T. Hecht, A. Weber, *Prepr. Petrol. Div. Am. Chem. Soc., 221st National Meeting, American Chemical Society, San Diego*, **2001**, 37–38.
[32] B. Wichterlová, N. Žilková, E. Uvarová, J. Čejka, Ch. Paganini, J. A. Lercher, *Appl. Catal. A* **1999**, *182*, 297–308.
[33] O. J. Kunkeler, B. J. Zuurdeeg, J. C. van der Waal, J. A. van Bokhoven, D. C. Koningsberger, H. van Bekkum, *J. Catal.* **1998**, *180*, 234–244.
[34] E. Bourgeat-Lami, P. Massiani, F. di Renzo, P. Espiau, F. Fajula, T. des Courieres, *Appl. Catal.* **1991**, *72*, 139–152.
[35] http://www.webelements.com.
[36] V. Umamaheswari, M. Hartmann, A. Pöppl, *J. Phys. Chem.* submitted.
[37] S. Ernst, M. Hunger, J. Weitkamp, *Chem. Ing. Tech.* **1997**, *6*, 77–79.
[38] B. Wichterlová, Z. Tvarůžková, Z. Sobalík, P. Sarv, *Microporous Mesoporous Mater.* **1998**, *24*, 223.
[39] C. A. Emeis, *J. Catal.* **1993**, *141*, 347–354.

Received: September 6, 2004

